

Synthesis and spectroscopic characterization of a hydride carbonyl ruthenium(II) complex with 2-methyl-4(5)nitroimidazole as a co-ligand

Jan Grzegorz Małecki, Anna Maroń*

Department of Crystallography, Institute of Chemistry, University of Silesia, 9th Szkolna St., 40-006 Katowice, Poland

ARTICLE INFO

Article history:

Received 2 January 2013

Accepted 20 February 2013

Available online 14 March 2013

Keywords:

Hydride carbonyl ruthenium(II) complexes

Imidazole derivatives

X-ray crystallography

DFT

Absorption and emission electronic spectra

Fluorescence

ABSTRACT

The reaction between $[\text{RuHCl}(\text{CO})(\text{PPh}_3)_3]$ and 2-methyl-4(5)-nitroimidazole (L) has been performed and the hydride carbonyl ruthenium(II) complex $[\text{RuH}(\text{CO})(\text{PPh}_3)_2(\text{L})]$ has been obtained by this reaction, running with deprotonation of the ligand. The molecular structure of the complex has been determined by X-ray crystallography and its spectroscopic characterization has been carried out by IR, ^1H , ^{31}P and ^{13}C NMR, UV–Vis spectroscopy. Supported by the DFT computational method, the electronic structure is described in order to explain the absorption and emission spectra obtained experimentally. The luminescence property of the complex has been examined and the quantum yield of the fluorescence has been obtained by a comparative method. The observable fluorescence is related to MLLCT excited states. The imidazole derivative ligand plays a role in the creation of the excited states.

© 2013 Elsevier Ltd. All rights reserved.

1. Introduction

Hydride carbonyl complexes of ruthenium(II) containing triphenylphosphine and N-heteroaromatic ligands derived from pyridine, imidazole and benzimidazole are one of the fastest growing areas in coordination chemistry, mainly due to its potential applications [1–5]. The wide interest in ruthenium(II) complexes as luminescence materials is a consequence of their application in photo-activated molecular systems [6–10]. In this regard, the attention of scientists is focused on designing spectroscopic properties by the introduction of specific ligands to the coordination sphere of the metal center. It is well known that in metal–ligand probes the heterocyclic ligands play a primary role in the determination of emissions originating from MLCT excited states. On the other hand, influences of the coordination environment can change the character of the excited state from MLCT to MLLCT [11]. Hence, one can see that not only the ligands directly related to the formed excited states have a significant effect, but the whole coordination environment of the central ions is important in this case. The hydride ligand is strong σ -donor and through the ‘trans effect’ affects neighboring ligands. Therefore, study on hydride carbonyl ruthenium(II) complexes seems to be of interest. Earlier we reported our study on ruthenium hydride carbonyl complexes with imidazole carboxylic acid derivative ligands [12]. For these complexes, emissions coming from MLCT excited states was observed and the nature of N-heterocyclic ligand had a substantial influence on the observed fluorescent properties.

In this paper, the synthesis and study by IR, NMR and UV–Vis spectroscopy and X-ray crystallography of a hydride carbonyl ruthenium(II) complex with 2-methyl-4(5)-nitroimidazole as a co-ligand are presented. Based on the crystal structure, computational research was made in order to determine the electronic structure of the complex by analysis of its optimized molecular geometry and its electronic population using the natural bond orbitals scheme. The latter was used to identify the nature of the interactions between the ligands and the central ion. The calculated density of states showed the interactions and influences of the orbital composition on the frontier electronic structure. Time dependent density functional theory (TD-DFT) was finally used to calculate the electronic absorption spectrum. Based on the molecular orbital scheme, the experimental absorption electronic spectrum has been interpreted. The luminescent property of the complex was examined and the quantum yields of the fluorescence were determined.

2. Experimental

$[\text{RuHCl}(\text{CO})(\text{PPh}_3)_3]$ was synthesized according to a literature method [13]. All other reagents used for the synthesis of the complex were commercially available and have been used without further purification.

2.1. Synthesis of the complex

The complex $[\text{RuH}(\text{CO})(\text{PPh}_3)_2(\text{L})]$ was synthesized by the reaction between $[\text{RuHCl}(\text{CO})(\text{PPh}_3)_3]$ (0.2 g, 2.0×10^{-4} mol) and

* Corresponding author. Tel.: +48 011323591886.

E-mail address: ank806@wp.pl (A. Maroń).

2-methyl-4(5)-nitroimidazole (0.028 g, 2.2×10^{-4} mol). The mixture of compounds was refluxed in methanol (60 mL) for 4 h. After this time, it was cooled and filtered. Crystals suitable for X-ray crystal analysis were obtained by slow evaporation of the reaction mixture.

IR (KBr, cm^{-1}): 3055 ν_{ArH} ; 2014 $\nu_{\text{Ru-H}}$; 1924 ν_{CO} ; 1501 $\nu_{\text{asym NO}_2}$; 1479 $\delta_{(\text{C-CH in the plane})}$; 1432 $\nu_{\text{Ph(P-Ph)}}$; 1365, 1350 $\nu_{\text{sym NO}_2}$; 1091 $\delta_{(\text{C-CH in the plane})}$; 743 $\delta_{(\text{C-C out of the plane})}$; 695 $\delta_{(\text{C-C in the plane})}$; 519 $\delta_{(\text{Ru-(H)CO})}$. UV-Vis (ethanol, nm (log ϵ): 433.6 (1.34), 347.4 (3.97), 274.0 (4.24), 208.2 (4.88). ^1H NMR (400 MHz, CDCl_3) δ : 7.73–7.65 (m, 1m); 7.59–6.87 (m, PPh₃), 3.50 (s, CH₃), –15.62 (t, $J = 19.8$ Hz, $\text{H}_{(\text{Ru})}$). ^{31}P NMR (162 MHz, CDCl_3) δ : 44.28 (s, PPh₃). ^{13}C NMR (CDCl_3) δ : 206.93 (s, C=O); 132.62, 132.10, 131.93, 128.50, 128.34 (1m, PPh₃); 77.04 (t, CDCl_3); 30.93 (s, CH₃).

2.2. Physical measurements

The infrared spectrum was recorded on a FT-IR Nicolet iS5 spectrophotometer in the spectral range 4000–400 cm^{-1} using a KBr pellet. The electronic spectrum was measured on a Lab Alliance UV-VIS 8500 spectrophotometer in the range 600–180 nm in ethanol solution. The ^1H , ^{31}P and ^{13}C NMR spectra were obtained at room temperature in CDCl_3 using a Bruker Avance 400 MHz spectrometer. Luminescence measurements were made in ethanolic solutions on a Hitachi F-7000 FL spectrophotometer at room temperature. The quantum yield of fluorescence was calculated using follow equation: $\Phi_s = \Phi_{\text{std}} \frac{\text{Grad}_s \eta_s^2}{\text{Grad}_{\text{std}} \eta_{\text{std}}^2}$, where Φ_s is the quantum yield of the unknown sample, Φ_{std} is the quantum yield of naphthalene, as a reference, at 313 nm and is equal to 0.21 [14], Grad_s and Grad_{std} are the gradients from the plots of the integrated fluorescence intensity vs the solution absorbencies at the excitation wavelength, and η_s and η_{std} are the refractive indices of the solvents. The samples were prepared with absorbencies less than 0.1 at the excitation wavelengths and were gradually diluted in order to minimize re-absorption effects and to avoid inner-filter effects, which may perturb the quantum yield values.

2.3. DFT calculations

The calculations were carried out using the GAUSSIAN09 [15] program. The molecular geometry of the singlet ground state of the complex was fully optimized in the gas phase at the B3LYP/DZVP level of theory [16,17]. For the complex a frequency calculation was carried out, verifying that the obtained optimized molecular structure corresponds to an energy minimum, thus only positive frequencies were expected. The DZVP basis set [18] with f functions with exponents 1.94722036 and 0.748930908 was used to describe the ruthenium atom and the basis set used for the lighter atoms (C, N, O, P, H) was 6-31G with a set of “d” and “p” polarization functions. The TD-DFT (time dependent density functional theory) method [19] was employed to calculate the electronic absorption spectrum of the complex in the solvent PCM (Polarizable Continuum Model) model. In this work 100 singlet excited states were calculated as vertical transitions for the complex. A natural bond orbital (NBO) analysis was also made for the complex using the NBO 5.0 package [20] included in GAUSSIAN09. Natural bond orbitals are orbitals localized on one or two atomic centers that describe the molecular bonding in a manner similar to a Lewis electron pair structure, and they correspond to an orthonormal set of localized orbitals of maximum occupancy. NBO analysis provides the contribution of atomic orbitals (s, p, d) to the NBO σ and π hybrid orbitals for bonded atom pairs. In this scheme, three NBO hybrid orbitals are defined, bonding orbital (BD), lone pair (LP) and core (CR), which were analyzed on the atoms directly bonded to or presenting some kind of interaction with the ruthenium atom. The contribution of a group (ligands, central ion) to a

molecular orbital was calculated using Mulliken population analysis. GAUSSSUM 2.2 [21] was used to calculate group contributions to the molecular orbitals and to prepare the partial density of states (DOS) spectrum. The DOS spectrum was created by convoluting the molecular orbital information with Gaussian curves of unit height and a FWHM (Full Width at Half Maximum) of 0.3 eV.

2.4. Crystal structure determination and refinement

A red crystal of $[\text{RuH}(\text{CO})(\text{PPh}_3)_2(\text{L})]$ was mounted on a Gemini A Ultra Oxford Diffraction automatic diffractometer equipped with a CCD detector, and used for data collection. X-ray intensity data were collected with graphite monochromated Mo $\text{K}\alpha$ radiation ($\lambda = 0.71073$ Å) at a temperature of 295.0(2) K, with the ω scan mode. Ewald sphere reflections were collected up to $2\theta = 50.10^\circ$. The unit cell parameters were determined from least-squares refinement of the setting angles of the 3853 strongest reflections for the studied complex. Details concerning crystal data and refinement are gathered in Table 1. Lorentz, polarization and empirical absorption corrections using spherical harmonics implemented in the SCALE3 ABSPACK scaling algorithm [22] were applied. The structure was solved by the Patterson method and subsequently completed by difference Fourier recycling. All the non-hydrogen atoms were refined anisotropically using the full-matrix, least-squares technique. The Ru–H hydrogen atom was found from difference Fourier synthesis after four cycles of anisotropic refinement and the remaining hydrogen atoms were refined as “riding” on the adjacent carbon atom with individual isotropic temperature factors equal to 1.2 times the value of the equivalent temperature factor of the parent atom. Bearing in mind the limitations of Fourier synthesis and the problems in recognizing artifacts in the immediate neighborhood of heavy atoms, it is doubtful whether a reliable position for the hydrogen atom bound to the Ru atom could be found in the difference Fourier map, avoiding the danger of mistaking the effects of the series termination errors for a true atomic position. In this complex the Ru–H bond length of

Table 1
Crystal data and structure refinement details of the $[\text{RuH}(\text{CO})(\text{PPh}_3)_2(\text{L})]$ complex.

	1
Empirical formula	$\text{C}_{41}\text{H}_{35}\text{N}_3\text{O}_3\text{P}_2\text{Ru}$
Formula weight	780.73
Temperature (K)	295.0(2)
Crystal system	orthorhombic
Space group	$P2_12_12_1$
Unit cell dimensions	
a (Å)	12.1794(5)
b (Å)	15.5281(7)
c (Å)	19.3642(7)
$\alpha = \beta = \gamma$ ($^\circ$)	90.00
Volume (Å ³)	3662.2(3)
Z	4
Calculated density (Mg/m^3)	1.418
Absorption coefficient (mm^{-1})	0.558
$F(000)$	1604
Crystal dimensions (mm)	$0.15 \times 0.11 \times 0.07$
θ range for data collection ($^\circ$)	3.35–25.05
Index ranges	$-14 \leq h \leq 14$, $-15 \leq k \leq 18$, $-23 \leq l \leq 23$
Reflections collected	12574
Independent reflections	$6220[R_{\text{int}}] = 0.0447$
Data/restraints/parameters	6220/0/456
Goodness-of-fit on F^2	1.088
Final R indices [$I > 2\sigma(I)$]	$R_1 = 0.0614$, $wR_2 = 0.0814$
R indices (all data)	$R_1 = 0.0974$, $wR_2 = 0.0940$
Largest diff. peak and hole	0.737/–0.573

1.67(5) Å does not deviate significantly from the bond length value located in the CSD 2013 basis. The OLEX2 [23], SHELXS97 and SHELXL97 [24] programs were used for all the calculations. Atomic scattering factors used were those incorporated in the computer programs.

3. Results and discussion

3.1. Spectroscopic characterization of the complex

The ^1H NMR spectrum of the complex shows a triplet at high field (-15.62 ppm), which indicates the presence of the hydride ligand coordinated to ruthenium central ion. The shift of the signal is due to the shielding effect of the metal and to the charge of the hydride ion. The range of the shift is characteristic for complexes with N,O-donor anionic ligands based on imidazole moieties and reflects the influence of the coordination environment on the interaction between the ruthenium central ion and the hydride ligand. The Ru–H signal is a triplet due to coupling with the two *trans* phosphorus atoms ($J_{\text{HP}} = 19.8$ Hz). Moreover, in the ^1H NMR spectrum of the complex a set of signals corresponding to the PPh_3 and 2-methyl-4(5)-nitroimidazole ligands are visible and are given in Section 2. Additionally, it is shown that there is a lack of signals coming from NH protons, that correlates with the molecular structure of $[\text{RuH}(\text{CO})(\text{PPh}_3)_2(\text{L})]$. In the ^{31}P NMR spectrum of the complex a singlet at 44.28 ppm is visible. It indicates the presence of magnetically equivalent phosphorus atoms, which proves the equivalence of the phosphine groups in the structure of the complex. The ^{13}C NMR spectrum presents signals attributed to PPh_3 and imidazole groups (see Section 2). Moreover, a signal at 206.93 ppm indicates the presence of the carbonyl group. The carbon from the methyl group of the imidazole derivative ligand gives a signal at 30.93 ppm.

The IR spectrum of the complex shows a strong $\text{C}\equiv\text{O}$ band at 1924 cm^{-1} and a Ru–H stretching band at 2014 cm^{-1} . In the parent complex, the ν_{CO} and $\nu_{\text{Ru-H}}$ stretching bands were observed at 1922 and 2020 cm^{-1} , respectively. For hydride carbonyl ruthenium(II) complexes with N,O-donor heteroaromatic ligands, the shift of the carbonyl stretching vibration in comparison to this mode for the parental complex is characteristic. It takes place when the N,O-donor ligand interacts with the ruthenium(II) center in such way that the delivery of electron density by backbonding to the carbonyl ligand is possible. In this case, the lack of a visible shift of ν_{CO} indicates that 2-methyl-4(5)-nitroimidazole is a rather weak ligand. The asymmetric and symmetric stretches of the NO_2 group give bands with maxima at 1501 and 1350 cm^{-1} , respectively, but the first band is partially covered by very strong $\delta_{(\text{C-CH in the plane})}$ bands related to triphenylphosphine groups present in the structure of the compound, and for this reason it is barely visible. The nitro group stretches in the free ligands are observed at 1505 and 1377 cm^{-1} and the visible change in the band position of the symmetric stretches of the NO_2 group indicates coordination of the nitro groups to ruthenium.

3.2. Molecular structure

The reaction between $[\text{RuHCl}(\text{CO})(\text{PPh}_3)_3]$ and 2-methyl-4(5)-nitroimidazole (L) results in red crystals of the title complex $[\text{RuH}(\text{CO})(\text{PPh}_3)_2(\text{L})]$, where L = 2-methyl-4(5)-nitroimidazole. The 2-methyl-4(5)-nitroimidazole ligand is coordinated to the ruthenium(II) central ion as a N,O-donor, with the removal of the imidazole NH proton. The deprotonation of the imidazole nitrogen atom is confirmed by the lack of signals coming from NH protons in the ^1H NMR spectrum. The complex crystallizes in the orthorhombic $P2_12_12_1$ space group and Fig. 1 presents the molecular structure of the complex (a structural drawing of the compound

is shown in Fig. 2). The experimental and calculated geometrical details as selected bond lengths and angles are listed in Table 2. The bond lengths and angles are comparable with distances in other hydride-carbonyl ruthenium(II) complexes with N-heteroaromatic ligands. In this complex the Ru–H bond distance of 1.67(5) Å does not differ significantly from the values for other ruthenium carbonyl hydride complexes found in the Cambridge Structural Database (CSD; ConQuest v. 1.15; 2013) and that found in the parent complex (1.7 Å) [25–28].

In the complex there is a pseudooctahedral coordination environment around the central ruthenium(II) ion. The largest deviation from an ideal octahedron comes from the bite angle of the 2-methyl-4(5)-nitroimidazole ligand. The N(1)–Ru(1)–O(2) angle is equal to $74.49(18)^\circ$. The carbonyl group lies in a *trans* position to the nitrogen heteroatom of the imidazole ring and the oxygen donor atom from nitro group is *trans* to the hydride ligand. The Ru(1)–C(1) and Ru(1)–H(1) bond lengths are equal to 1.829(7) and 1.67(5) Å, respectively. Moreover, the C(1)–O(1) bond and the Ru(1)–C(1)–O(1) angle are equal to 1.158(7) Å and 179.16° . The Ru–C bond distance is normal for a monomeric Ru(II) carbonyl complex (the distances generally range from 1.74 to 1.98 Å). In the complex, the phosphine ligands are in a *trans* conformation, with the P(1)–Ru(1)–P(2) angle being equal to $175.92(6)^\circ$. Generally, the presence of a singlet in the ^{31}P NMR spectrum of such a complex shows the equivalence of the triphenylphosphine ligands.

3.3. Electronic structures

The ground state geometry of the complex was optimized in the singlet state using the B3LYP functional. The calculation was carried out for a gas phase molecule and in general the predicted bond lengths and angles are over-estimated by about 0.1 Å and 4° , respectively. The calculated IR frequencies of the complex show agreement with the experimental spectrum; the differences can be explained by the neglect of intermolecular interactions for the gas phase. From the data collected in Table 2, one may see that the major difference between the experimental and calculated geometries is found in the Ru(1)–C(1) distance (0.15 Å).

Based on the optimized geometry of the complex, an NBO analysis was performed in order to reveal the nature of the coordination between the ruthenium center and the donor atoms of the

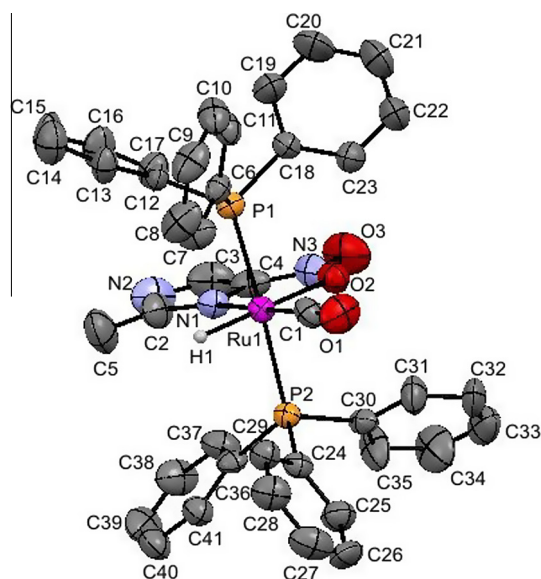


Fig. 1. Molecular structure of the $[\text{RuH}(\text{CO})(\text{PPh}_3)_2(\text{L})]$ complex. Hydrogen atoms (bonding with carbons) are omitted for clarity.

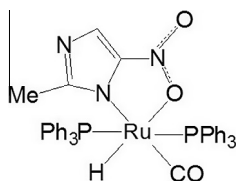


Fig. 2. Structural drawing of the $[\text{RuH}(\text{CO})(\text{PPh}_3)_2(\text{L})]$ complex.

Table 2

Selected bond lengths (Å) and angles ($^\circ$) for the $[\text{RuH}(\text{CO})(\text{PPh}_3)_2(\text{L})]$ complex with the optimized geometry values.

	Exp	Cal
<i>Bond lengths (Å)</i>		
Ru(1)–C(1)	1.829(7)	1.875
Ru(1)–N(1)	2.116(5)	2.164
Ru(1)–O(2)	2.254(4)	2.274
Ru(1)–P(2)	2.3608(15)	2.433
Ru(1)–P(1)	2.3640(15)	2.433
Ru(1)–H(1)	1.67(5)	1.607
O(1)–C(1)	1.158(7)	1.162
<i>Angles ($^\circ$)</i>		
C(1)–Ru(1)–N(1)	175.3(2)	173.82
C(1)–Ru(1)–O(2)	100.8(2)	99.92
N(1)–Ru(1)–O(2)	74.49(18)	73.90
C(1)–Ru(1)–P(2)	88.4(2)	89.54
N(1)–Ru(1)–P(2)	91.09(14)	90.88
O(2)–Ru(1)–P(2)	91.06(11)	93.93
C(1)–Ru(1)–P(1)	90.8(2)	89.54
N(1)–Ru(1)–P(1)	90.03(14)	90.87
O(2)–Ru(1)–P(1)	93.02(11)	93.93
P(2)–Ru(1)–P(1)	175.92(6)	172.13
C(1)–Ru(1)–H(1)	89.3(16)	89.44
N(1)–Ru(1)–H(1)	95.4(16)	96.73
O(2)–Ru(1)–H(1)	169.4(16)	170.63
P(2)–Ru(1)–H(1)	86.1(15)	86.09
P(1)–Ru(1)–H(1)	89.9(15)	86.09
O(1)–C(1)–Ru(1)	179.1(6)	178.22

ligands. The interactions between the ligands and the central ion manifest themselves in the charge on the complex metal ion. The metal ion in the complex is formally in the +2 oxidation state, but in the studied complex the calculated natural charge is considerably lower than +2, being equal to -0.786 . This indicates that the donations from the ligands to the central ion have the advantage over the back donations from the metal to the ligands. The NBO analysis (*Second Order Perturbation Theory Analysis of the Fock Matrix in NBO Basis*) also shows that the donation from the 2-methyl-4(5)-nitroimidazole ligand to the ruthenium central ion, with value of 347.41 kcal/mol, exceeds the back donation, equal to 33.52 kcal/mol. In addition to the σ -donor properties, this ligand exhibits weak π -acceptor properties. The analysis shows that the imidazole derivative N,O-donor ligand does not show covalent bonding with ruthenium; the Coulomb-type interaction between the ruthenium center and the ligand is clearly visible in the calculated Wiberg bond indexes, which are considerably lower than one. The Ru–N and Ru–O bond indices are equal to 0.44 and 0.34, respectively. The Ru–P bond orders are also smaller than 1 and are close to 0.70. The charge of the hydride ligands is +0.06 and the Wiberg index of the Ru–H bond is equal to 0.81. The charge on the carbonyl group, calculated by summing the individual charges on the carbon and oxygen atoms, is 0.20 for the complex. The Wiberg index of the CO bond in the complex is reduced by about 0.18 with respect to free CO ($W_{\text{CO}} = 2.23$).

Analysis of the frontier molecular orbitals is useful for understanding spectroscopic properties, such as electronic absorption and emission spectra. The density of state (DOS) and overlap population density-of-states (OPDOS) in terms of Mulliken population

analysis were calculated using the GAUSSSUM program, and Fig. 3 presents the composition of the fragment orbitals contributing to the molecular orbitals of the complex. In the HOMO orbital of the complex, d_{Ru} orbitals and orbitals of the 2-methyl-4(5)-nitroimidazole ligand participate in the same range (43%). The contribution of the PPh_3 ligands is also visible, with a 14% share in this orbital. The contribution of d_{Ru} orbitals in lower occupied orbitals is visible for the HOMO–1 to HOMO–4 orbitals (23–78%). For these orbitals the participation of the carbonyl ligand is observed at about 15%. In the unoccupied (LUMO) orbitals of the complex the triphenylphosphine ligands play a significant role, but the LUMO is localized on the imidazole derivative ligand (95%). The d orbitals of the ruthenium ion share in LUMO+1, LUMO+4 and LUMO+9 orbitals at the level of 16–19%. On the OPDOS plot the antibonding interaction between the imidazole ligand and the ruthenium(II) central ion in the frontier HOMO orbitals is visible. On the other hand, in this energy range, the influence of the carbonyl ligand on the ruthenium d orbitals has a positive value, indicating a bonding character of these interactions.

3.4. Electronic absorption and emission spectra

The electronic absorption spectrum was measured on a Lab Alliance UV–VIS 8500 spectrophotometer in the range 500–180 nm in methanol solution. The experimental spectrum of the complex

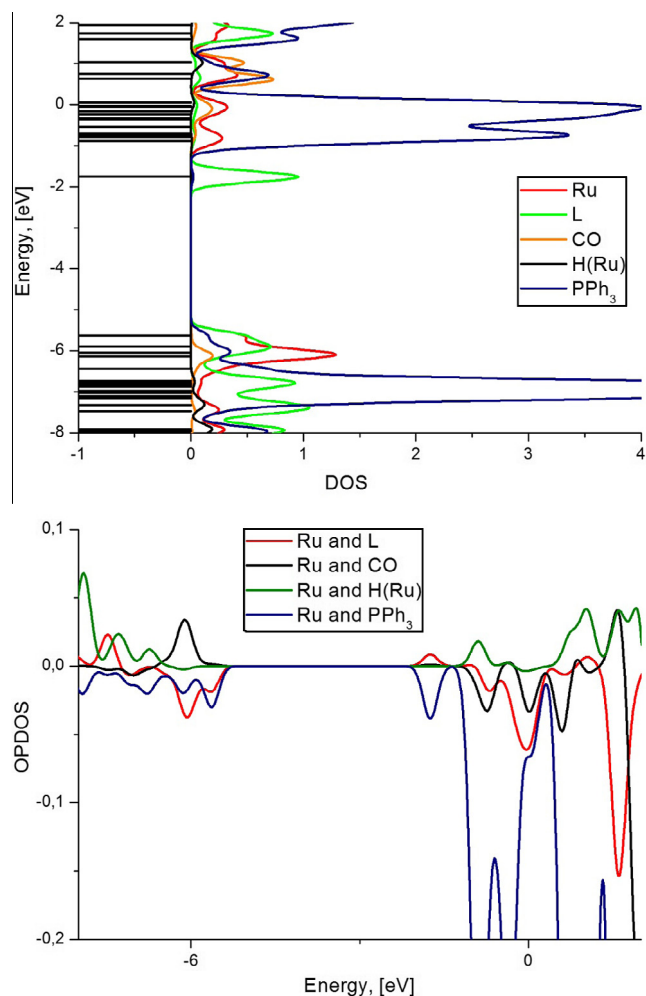


Fig. 3. The density-of-states and overlap partial density of states diagrams for interactions between the ruthenium central ion and the ligands in the complex $[\text{RuH}(\text{CO})(\text{PPh}_3)_2(\text{L})]$.

Table 3
The electronic transitions for the complex calculated with the B3LYP functional by the TD-DFT method.

Wavelength (nm)	<i>f</i>	Transitions	Character	Exp (nm)
411.55	0.0627	HOMO → LUMO (96%)	$d_{Ru} \rightarrow \pi^*_L$	433.6
379.77	0.0024	H-2 → LUMO (76%), H-1 → LUMO (18%)	$d_{Ru} \rightarrow \pi^*_L$	
373.13	0.0002	H-3 → LUMO (99%)	$d_{Ru} \rightarrow \pi^*_L$	
342.95	0.0265	H-4 → LUMO (26%), H-2 → LUMO (22%), H-1 → LUMO (50%)	$d_{Ru} \rightarrow \pi^*_L$	347.4
311.75	0.0879	H-4 → LUMO (64%), H-1 → LUMO (24%)	$d_{Ru}/\pi_L \rightarrow \pi^*_L$	
298.45	0.1096	H-2 → L+1 (43%), H-1 → L+1 (22%)	$d_{Ru}/\pi_L \rightarrow \pi^*_{PPh_3}$	274.0
279.81	0.0187	HOMO → L+2 (32%), HOMO → L+3 (64%)	$d_{Ru}/\pi_L \rightarrow \pi^*_{PPh_3}$	
276.42	0.0144	HOMO → L+4 (71%)	$d_{Ru}/\pi_L \rightarrow \pi^*_{PPh_3}/d_{Ru}$	
270.85	0.0573	H-2 → L+1 (24%), H-1 → L+1 (67%)	$d_{Ru} \rightarrow \pi^*_{PPh_3}$	250.2
268.01	0.0252	HOMO → L+5 (85%)	$d_{Ru}/\pi_L \rightarrow \pi^*_{PPh_3}$	
257.16	0.3115	H-4 → L+1 (51%), H-2 → L+1 (11%)	$d_{Ru}/\pi_L \rightarrow \pi^*_{PPh_3}$	
247.09	0.0014	HOMO → L+9 (84%)	$d_{Ru}/\pi_L \rightarrow \pi^*_{PPh_3}/d_{Ru}$	
233.69	0.0121	HOMO → L+13 (61%)	$\pi_L \rightarrow \pi^*_{PPh_3}$	
225.07	0.0062	H-9 → L+2 (35%), H-4 → L+5 (26%)	$\pi_{PPh_3} \rightarrow \pi^*_{PPh_3}$	208.2

shows maxima of absorption at 433.6, 347.4, 274.0 and 208.2 nm. The theoretical absorption spectrum of the complex was obtained from the calculations of the singlet excited states by the TD-DFT method. Computation of 100 excited states of the complex allowed for the interpretation of the experimental spectrum. The selected excited states and their assignment to the absorption bands are shown in Table 3. The bands above 300 nm have HOMO/H-1/H-2 → LUMO character. Taking into account the fact that the *d* ruthenium orbitals play a role in these HOMOs, and the LUMO orbital is localized on the imidazole derivative ligand, the transitions at 433.6 and 347.4 nm have *Metal-Ligand Charge Transfer* character. However, given that the triphenylphosphine ligands mainly participate in the LUMOs and due to the contribution of both ruthenium *d* orbitals and π bonding orbitals of the imidazole ligand in the frontier HOMO orbital, the bands observed at 274 and 250 nm have been assigned to *MLLCT* transitions ($d_{Ru}/\pi_L \rightarrow \pi^*_{PPh_3}$), with a small admixture of *d-d* character. The highest experimental band, close to 210.0 nm, may result from transitions in the PPh_3 ligands.

The fluorescence spectrum of the complex has been prepared in optically diluted (O.D. < 0.1) ethanolic solution at room temperature. The measurement of the quantum yield has been examined

in optically diluted solutions by the comparative method, using naphthalene in ethanol as a standard ($\Phi_{ST} = 0.21$). The solution of the complex has been excited at a wavelength equal to 274 nm and the emission maximum was observed at 307 nm. The Stokes shift is equal to 3923.06 cm^{-1} . The excitation band corresponds to the transition $d_{Ru}/\pi_L \rightarrow \pi^*_{PPh_3}/d_{Ru}$ for the absorption spectrum of the complex. The assignments are supported by the analysis of the frontier orbitals of the complex, showing a partial contribution of ligand nature. As one can see from Table 3, the transitions calculated in this energy range have *MLLCT* character and proceed between the frontier HOMOs and LUMO+1 orbital. On the formation of excited states, both the metal ion and the imidazole derivative ligand are involved. In the formed excited states, a wide share of the triphenylphosphine ligands is visible with an admixture of ruthenium *d* orbitals and a slight contribution of the imidazole derivative ligand. At high optical dilution (O.D. < 0.03), the excitation band at 318 nm is visible with an emission maximum at 361 nm. This excitation band has *MLCT* character and proceeds between the frontier HOMOs and LUMO orbital. In the formed excited states a contribution of the imidazole derivative ligand is dominant. The Stokes shift in this case is equal to 3745.71 cm^{-1} . Moreover, the observed fluorescence properties are also related

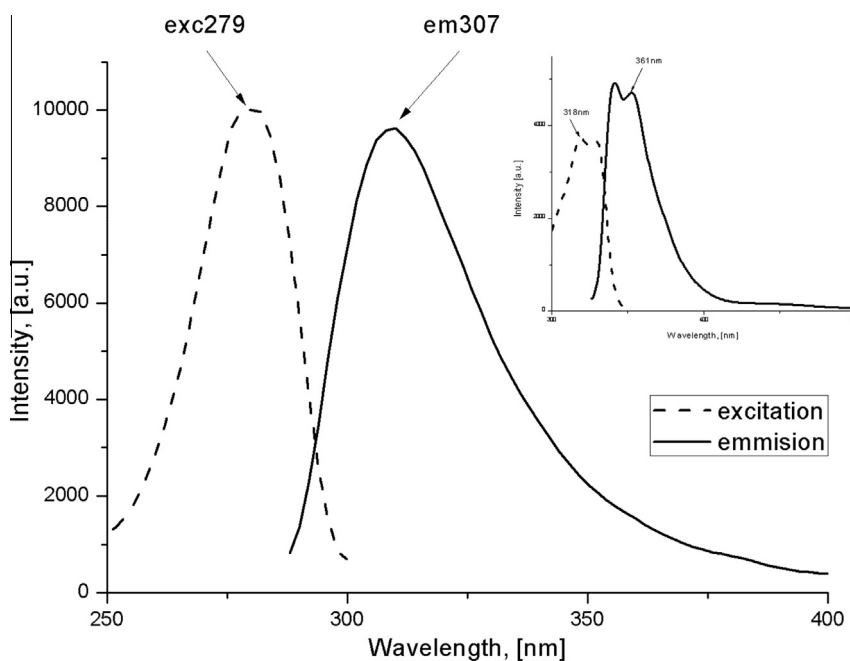


Fig. 4. Emission spectrum of the $[RuH(CO)(PPh_3)_2(L)]$ complex in methanolic solution.

to the fact that in the frontier HOMOs of the complex, the carbonyl ligand plays a significant role and strong luminescence results in its participation in the formation of excited states. The excitation and the emission spectra of the complex are given in Fig. 4. The quantum efficiency is equal to 0.23. The value of the quantum efficiency of fluorescence for this complex may be correlated with the fact that there is no clear participation of one fragment of the molecular orbital in the excited state, which suggests that more than one excited state plays a role in the emission band.

4. Conclusions

The hydride carbonyl complex of ruthenium(II) with 2-methyl-4(5)-nitroimidazole as a co-ligand was synthesized. The complex was characterized by infra red, nuclear magnetic resonance, electronic absorption and emission spectroscopy, and by X-ray crystallography. The electronic structure of the complex was determined using the density functional theory (DFT) method, employed for discussion of its properties and used to analyze the UV–Vis spectrum. The imidazole derivative ligand reacts as an N,O-donor ligand with deprotonation of the NH imine proton. The presented luminescence properties of the complex strictly depend on its electronic structure, and on the formation of excited states, the contribution and the nature of the ligands are respectively very substantial and important. In this complex the fluorescence originates from excited states described as MLLCT (Metal-to-Ligand-to-Ligand Charge Transfer), as distinguished from previously investigated complexes with imidazole carboxylic acid derivative ligands.

Acknowledgements

The GAUSSIAN-09 calculations were carried out in the Wrocław Centre for Networking and Supercomputing, WCSS, Wrocław, Poland, <http://www.wcss.wroc.pl>, under calculational Grant No. 18.

Appendix A. Supplementary data

CCDC 917237 contains the supplementary crystallographic data for [RuH(CO)(PPh₃)₂(L)]. These data can be obtained free of charge via <http://www.ccdc.cam.ac.uk/conts/retrieving.html>, or from the Cambridge Crystallographic Data Centre, 12 Union Road, Cambridge CB2 1EZ, UK; fax: (+44) 1223-336-033; or e-mail: deposit@ccdc.cam.ac.uk.

References

- [1] S. Kannan, M. Sivagamasundari, R. Ramesh, Yu Liu, J. Organomet. Chem. 693 (2008) 2251.
- [2] M. Sivagamasundari, R. Ramesh, Spectrochim. Acta, Part A 67 (2007) 256.
- [3] M. Sivagamasundari, R. Ramesh, Spectrochim. Acta, Part A 66 (2007) 427.
- [4] M.V. Kaveri, R. Prabhakaran, R. Karvembu, K. Natarajan, Spectrochim. Acta, Part A 61 (2005) 2915.
- [5] M. Ulaganatha Raja, N. Gowri, R. Ramesh, Polyhedron 29 (2010) 1175.
- [6] A. Harriman, A. Khatyr, R. Ziessel, Res. Chem. Intermed. 33 (2007) 49.
- [7] P. Wang, R. Humphry-Baker, J.E. Moser, S.M. Zakeeruddin, M. Grätzel, Chem. Mater. 16 (2004) 3246.
- [8] Y. Sun, S.N. Collins, L.E. Joyce, C. Turro, Inorg. Chem. 49 (2010) 4257.
- [9] J.-F. Yin, J.-G. Chen, Z.-Z. Lu, K.-C. Ho, H.-C. Lin, K.-L. Lu, Chem. Mater. 22 (2010) 4392.
- [10] S. Deng, G. Krueger, P. Taranekar, S. Sriwichai, R. Zong, R.P. Thummel, R.C. Advincula, Chem. Mater. 23 (2011) 3302.
- [11] D.J. Stufkens, A. Vičėk Jr., Coord. Chem. Rev. 177 (1998) 137.
- [12] J.G. Matecki, A. Maroń, S. Krompiec, M. Filapek, M. Penkala, B. Marcol, Polyhedron 49 (2013) 190.
- [13] N. Ahmad, J.J. Levinson, S.D. Robinson, M.F. Uttely, Inorg. Synth. 15 (1974) 48.
- [14] C.A. Parker, T.A. Joyce, Trans. Faraday Soc. 62 (1966) 2785.
- [15] M.J. Frisch, G.W. Trucks, H.B. Schlegel, G.E. Scuseria, M.A. Robb, J.R. Cheeseman, G. Scalmani, V. Barone, B. Mennucci, G.A. Petersson, H. Nakatsuji, M. Caricato, X. Li, H.P. Hratchian, A.F. Izmaylov, J. Bloino, G. Zheng, J.L. Sonnenberg, M. Hada, M. Ehara, K. Toyota, R. Fukuda, J. Hasegawa, M. Ishida, T. Nakajima, Y. Honda, O. Kitao, H. Nakai, T. Vreven, J.A. Montgomery Jr., J.E. Peralta, F. Ogliaro, M. Bearpark, J.J. Heyd, E. Brothers, K.N. Kudin, V.N. Staroverov, R. Kobayashi, J. Normand, K. Raghavachari, A. Rendell, J.C. Burant, S.S. Iyengar, J. Tomasi, M. Cossi, N. Rega, J.M. Millam, M. Klene, J.E. Knox, J.B. Cross, V. Bakken, C. Adamo, J. Jaramillo, R. Gomperts, R.E. Stratmann, O. Yazyev, A.J. Austin, R. Cammi, C. Pomelli, J.W. Ochterski, R.L. Martin, K. Morokuma, V.G. Zakrzewski, G.A. Voth, P. Salvador, J.J. Dannenberg, S. Dapprich, A.D. Daniels, O. Farkas, J.B. Foresman, J.V. Ortiz, J. Cioslowski, D.J. Fox, GAUSSIAN 09, Revision A.1, Gaussian, Inc., Wallingford, CT, 2009.
- [16] A.D. Becke, J. Chem. Phys. 98 (1993) 5648.
- [17] C. Lee, W. Yang, R.G. Parr, Phys. Rev. B 37 (1988) 785.
- [18] K. Eichkorn, F. Weigend, O. Treutler, R. Ahlrichs, Theor. Chim. Acc. 97 (1997) 119.
- [19] M.E. Casida, in: J.M. Seminario (Ed.), Recent Developments and Applications of Modern Density Functional Theory, Theoretical and Computational Chemistry, vol. 4, Elsevier, Amsterdam, 1996, p. 391.
- [20] E.D. Glendening, A.E. Reed, J.E. Carpenter, F. Weinhold, NBO (version 3.1).
- [21] N.M. O'Boyle, A.L. Tenderholt, K.M. Langner, J. Comput. Chem. 29 (2008) 839.
- [22] CRYSLIS RED, Oxford Diffraction Ltd., Version 1.171.29.2.
- [23] O.V. Dolomanov, L.J. Bourhis, R.J. Gildea, J.A.K. Howard, H. Puschmann, J. Appl. Crystallogr. 42 (2009) 339.
- [24] G.M. Sheldrick, Acta Crystallogr., Sect. A 64 (2008) 112.
- [25] M. Chandra, A.N. Sahay, D.S. Pandey, M.C. Puerta, P. Valerga, J. Organomet. Chem. 648 (2002) 39.
- [26] M. Trivedi, M. Chandra, D.S. Pandey, M.C. Puerta, P. Valerga, J. Organomet. Chem. 689 (2004) 879.
- [27] T.K. Mondal, J. Dinda, J. Cheng, T.-H. Lu, C. Sinha, Inorg. Chim. Acta 361 (2008) 2431.
- [28] H. Adams, A.M. Coffey, M.J. Morris, Inorg. Chim. Acta 363 (2010) 173.